DOI: 10.1111/ede.12239

RESEARCH

WILEY

The development of the cucullaris muscle and the branchial musculature in the Longnose Gar, (*Lepisosteus osseus*, Lepisosteiformes, Actinopterygii) and its implications for the evolution and development of the head/trunk interface in vertebrates

Benjamin Naumann[1] | **Peter Warth**[1] | **Lennart Olsson**[1] | **Peter Konstantinidis**[2]

[1] Institut für Spezielle Zoologie und Evolutionsbiologie mit Phyletischem Museum, Friedrich-Schiller-Universität, Jena, Germany

[2] Department of Fisheries and Wildlife, Oregon State University, Corvallis, Oregon

Correspondence
Benjamin Naumann, Institut für Spezielle Zoologie und Evolutionsbiologie mit Phyletischem Museum, Friedrich-Schiller-Universität, Jena, Germany.
Email: benjamin.naumann@uni-jena.de

Funding information
Volkswagen Foundation, Grant number: I84/825

The vertebrate head/trunk interface is the region of the body where the different developmental programs of the head and trunk come in contact. Many anatomical structures that develop in this transition zone differ from similar structures in the head or the trunk. This is best exemplified by the cucullaris/trapezius muscle, spanning the head/trunk interface by connecting the head to the pectoral girdle. The source of this muscle has been claimed to be either the unsegmented head mesoderm or the somites of the trunk. However most recent data on the development of the cucullaris muscle are derived from tetrapods and information from actinopterygian taxa is scarce. We used classical histology in combination with fluorescent whole-mount antibody staining and micro-computed tomography to investigate the developmental pattern of the cucullaris and the branchial muscles in a basal actinopterygian, the Longnose gar (*Lepisosteus osseus*). Our results show (1) that the cucullaris has been misidentified in earlier studies on its development in *Lepisosteus*. (2) Cucullaris development is delayed compared to other head and trunk muscles. (3) This developmental pattern of the cucullaris is similar to that reported from some tetrapod taxa. (4) That the retractor dorsalis muscle of *L. osseus* shows a delayed developmental pattern similar to the cucullaris. Our data are in agreement with an explanatory scenario for the cucullaris development in tetrapods, suggesting that these mechanisms are conserved throughout the Osteichthyes. Furthermore the developmental pattern of the retractor dorsalis, also spanning the head/trunk interface, seems to be controlled by similar mechanisms.

1 | INTRODUCTION

The vertebrate head is often regarded as a discrete developmental unit, distinct from the trunk and governed by a different developmental program (Ericsson, Knight, & Johanson, 2013; Kuratani, 2008; Theis et al., 2010). The region of the vertebrate body where these distinct units, the head and the trunk, meet is termed the head/trunk interface (Kuratani, 1997). The evolution and development of the vertebrate head/trunk interface have attracted much less attention compared to the head and trunk on their own. However, with the advent of new methods the interest in this

transition area increased rapidly (Epperlein, Khattak, Knapp, Tanaka, & Malashichev, 2012; Ericsson et al., 2013; Huang, Zhi, Patel, Wilting, & Christ, 2000; Kuratani, 2008; Matsuoka et al., 2005; Oisi, Fujimoto, Ota, & Kuratani, 2015; Piekarski & Olsson, 2007; Sefton, Bhullar, Mohaddes, & Hanken, 2016; Tada & Kuratani, 2015; Theis et al., 2010; Trinajstic et al., 2013). The interface between the head and the trunk is defined by the posterior-most population of cephalic neural crest cells and can be demarked by an s-shaped curve outlined by the vagal nerve dorsally and the spinal hypoglossal nerve ventrally (Kuratani, 1997). The development of the muscles (Kuratani, 2008), nerves (Tada & Kuratani, 2015), and the skeleton (Gegenbaur, 1889) of the head/trunk interface differ from those of the head and trunk by often showing a combination of head and trunk features (Ericsson et al., 2013). This is exemplified by the enigmatic cucullaris muscle. The cucullaris, and its amniote homolog the trapezius muscle (Edgeworth, 1935; Gegenbaur, 1889), spans across the head/trunk interface from its origin at the occiput to its insertion on the shoulder girdle. Based on anatomical and developmental evidence, its affiliation to either the head (Edgeworth, 1935) or the trunk (Couly, Coltey, & Le Douarin, 1993; Huang et al., 2000; Noden, 1983; Piekarski & Olsson, 2007) is controversially debated.

The innervation and embryonic origin of muscles are used as classical evidence in assessing homology. The sternohyoideus muscle for example is of somitic origin and starts forming in the trunk before migrating into the head. Its somitic origin can however still be inferred in adults, as it retains its original spinal innervation (Edgeworth, 1935). The cucullaris in non-amniote vertebrates is always innervated by a single ramus (sometimes called the ramus accessorius) of the vagal nerve (Edgeworth, 1935; Fürbringer, 1874; Gegenbaur, 1889). In contrast, in amniotes this branch is often treated as a discrete nerve (accessory nerve). In some taxa the cucullaris becomes additionally innervated by the anterior spinal nerves (Edgeworth, 1935; Ericsson et al., 2013), which might be due to the elongated neck in these taxa.

Another argument about the origin of the cucullaris muscle is based on its interaction with the cranial neural crest. The cranial neural crest is necessary for the differentiation of cranial muscles but has no influence on somite-derived trunk muscles (Ericsson, Cerny, Falck, & Olsson, 2004). A neural crest contribution to the connective tissue surrounding the cucullaris has been reported for two amniote taxa, chicken (Couly et al., 1993) and mouse (Matsuoka et al., 2005), but could not be confirmed in the non-amniote axolotl (Epperlein et al. 2012). Despite the contradicting data there are some consistent characters of the cucullaris muscle across vertebrates. First, it is governed by the head myogenic program (Sefton et al., 2016; Theis et al., 2010) and second, its delayed differentiation in respect to all other muscles in the head or trunk (Edgeworth, 1935; Noden, 1983; Piekarski & Olsson, 2007; Theis et al., 2010; Ziermann & Diogo, 2013). A possible explanation for the peculiar developmental pattern of this muscle has been proposed by Theis et al. (2010), who argues that the crossing of the head/trunk interface exposes the cucullaris to the trunk myogenic program, delaying its differentiation.

However, most of the recent data are derived from model organisms such as axolotl (Piekarski & Olsson, 2007; Sefton et al., 2016), chicken (Huang et al., 2000; Theis et al., 2010) and mouse (Matsuoka et al., 2005). Consequently, the focus is shifted toward the tetrapod taxa. However, to understand the evolutionary history of the cucullaris and to address the controversy of its origin it is important to study a wider variety of taxa of different phylogenetic affiliations. Basal actinopterygians are of special interest as they presumably reflect a more ancestral condition than tetrapods, and in some characters show more basal character states than chondrichthyans (Zhu et al., 2016). Additionally some actinopterygians (e.g., lepisosteids) possess another muscle that is of special interest, the retractor dorsalis (Edgeworth, 1911). As the cucullaris, the retractor dorsalis of lepisosteids develops in the head trunk interface, is innervated by the vagal nerve and has been claimed to be derived from the anterior-most somites (Edgeworth, 1911) or head mesoderm (Edgeworth, 1929). Lepisosteids therefore are a suitable model to study these two muscles side by side and to evaluate the hypothesis of Theis et al. (2010) (see above). In this study, we approach this topic from a morphological view and investigate the developmental pattern of the cucullaris and the retractor dorsalis in relation to the branchial and the hypobranchial muscles in *Lepisosteus osseus.*

2 | MATERIALS AND METHODS

2.1 | Specimens

Specimens were collected on the Mattaponi River (Virginia) in 2013–2015 and preserved in 4% buffered paraformaldehyde at 4°C overnight before transferred to 70% ethanol for long-term storage. Staging of the embryos and larvae follows Long and Ballard (2001). All specimens are listed in Table 1.

2.2 | Terminology

For the terminology of the muscles we follow mainly the terminology used for Teleostei (Winterbottom, 1974) except for the protractor pectoralis and adductor arcus branchialium 4. For these muscles we use the terms cucullaris, instead of protractor pectoralis, and attractor arcus branchialium, instead of adductor arcus branchialium 4 according to Edgeworth (1935).

TABLE 1 List of specimens

Stage (Long & Ballard, 2001)	Length (SL,NL)	Specimen number	Method	VIMS number
27	n.A.	Lo023	FWAB	VIMS 310345
28	5.9 mm NL	Lo001	FWAB	VIMS 22688
29	7.2 mm NL	Lo002	FWAB	VIMS 22688
30	8.3 mm NL	Lo003	FWAB	VIMS 22688
31	9.5 mm NL	Lo004	FWAB	VIMS 22688
31	9.3 mm NL	Lo016	FWAB	VIMS 22688
31	9.7 mm NL	Lo005	FWAB	VIMS 22688
32	10.9 mm NL	Lo006	FWAB	VIMS 22688
32	10.7 mm NL	Lo017	FWAB	VIMS 22688
33	13.6 mm NL	Lo007	FWAB	VIMS 22688
34	16.1 mm SL	Lo008	FWAB	VIMS 22688
Juvenile	20.0 mm SL	Lo009	FWAB	VIMS 22688
Juvenile	21.0 mm SL	Lo011	FWAB	VIMS 22688
Juvenile	22.0 mm SL	Lo012	FWAB	VIMS 22688
Juvenile	24.0 mm SL	Lo010	FWAB	VIMS 22688
Juvenile	23.0 mm SL	Lo030	FWAB + AR	VIMS 31040
31/32	11.0 mm NL	LoSec001	His	n.A.
33	14.0 mm NL	LoSec002	His	n.A.
34	16.0 mm NL	LoSec003	His	n.A.
Juvenile	21.0 mm NL	LoSec004	His	n.A.
Juvenile	27.0 mm NL	LoSec005	His	n.A.
31/32	10.0 mm SL	n.A.	μCT	VIMS 22684
32	12.8 mm NL	n.A.	μCT	VIMS 22685
34	16.1 mm SL	n.A.	μCT	VIMS 22686
Juvenile	22.0 mm SL	n.A.	μCT	VIMS 22687

FWAB, fluorescent whole-mount antibody staining, FWAB + AR, FWAB and alizarin red; His, Azan-stained histological sections; n.A., not available; NL, normal length; SL, standard length; μCT, micro-computed tomography.

2.3 | Histology

Specimens were embedded in paraffin, sectioned at 8 μm in transverse orientation and stained after Heidenhain-Azan (Böck, 1989). Sections were digitalized with an Olympus BX51 microscope using the dotslide software 2.3 (Olympus Corporation, Tokyo, Japan).

2.4 | CT scan

For a μCT scan and subsequent 3D reconstruction, a 22.0 mm juvenile gar was treated with phosphotungstic acid according to the procedure described earlier (Metscher, 2009). The specimen was scanned with an X-radia XCT scanner.

2.5 | Immunohistochemistry

Specimens were post-fixed in Dent's fixative and bleached in Dent's bleach. Antibody staining was conducted on whole mounts according to standard protocols (Klymkowsky & Hanken, 1991) using monoclonal 12/101 (Developmental Studies Hybridoma Bank, diluted), or a combination of anti-desmin (Monosan, PS031) and anti-acetylated alpha-tubulin (Sigma–Aldrich, Darmstadt, Germany, T6793) primary antibodies at dilutions of 1:100 (12/101, anti-desmin) and 1:500 (anti-acetylated alpha tubulin) respectively in DAKO antibody diluent. Alexa 488 and Alexa 568 (Thermo Scientific, Darmstadt, Germany) were used as secondary antibodies at 1:200. Clearing was done using BABB (benzyl alcohol/benzyl benzoate, 2/1). To look at the connection of muscles to the bony pectoral girdle, a whole-mount specimen stained with an antibody against desmin was incubated with 0,01% Alizarin red in PBS overnight and cleared with BABB.

2.6 | Image acquisition and processing

Virtual sections of whole mounts were taken with a ZEISS LSM 510. 3D reconstructions on the basis of μCT and clsm scans were performed using Amira 5.2 (FEI Visualization

Sciences Group, Bordeaux, France) and transferred to MAYA software (Autodesk GmbH, Munich, Germany) for visualization purposes. Background cleaning, contrast enhancement and color saturation of all images were adjusted using Adobe Photoshop CS6.

3 | RESULTS

3.1 | Development of the hypobranchial musculature

In *L. osseus*, the hypobranchial musculature is represented solely by the sternohyoideus muscle (rectus cervicis muscle in Edgeworth, 1935). It inserts on the hypohyal via a strong tendon anteriorly (Figures 1a and 1b). Posteriorly, it is first attached to the scapulocoracoid until stage 32 but changes to the cleithrum at stage 33 and, in part, becomes continuous with the hypaxonic trunk musculature in older larvae (Figures 1a and 1b).

At stage 30, the sternohyoideus muscle appears at the anterior end of the yolk sac, ventral to the branchial arches and dorsal to the heart. It is sub-divided into three distinct segments (Figure 1c, white arrows). The sternohyoideus is slightly curved posteriorly and not attached to any skeletal elements.

At stage 31, the muscle is elongated compared to the previous stage but neither its posterior nor its anterior end is attached to the corresponding skeletal element as it is described in older stages (Figure 1d). It is sub-divided into three to four (depicted specimen) distinct segments, while the anterior-most segment is smaller compared to the three subsequent segments (Figure 1d, gray arrows).

At stage 32, the sternohyoideus has extended farther anteriorly (Figure 1e), and its anterior end tapers into a tendon that attaches to the hypohyal cartilage. The posterior end of the muscle inserts on the scapulocoracoid, embracing the dorsal quarter of the heart together with its antimere (Figure 1e).

At stage 33, the posterior insertion of the sternohyoideus is now on the ossifying cleithrum, showing the juvenile/adult condition (Figure 1b). The posterior ends of the left sternohyoideus encase the ventral half of the heart now, which is due to the elongation of the snout and the consumption of the yolk sac (Figure 1f),

3.2 | Development of the ventral branchial muscles

At stage 29 (Figures 2a and 2a′), regions with higher levels of autofluorescence indicate formation of branchial arches 1–3 (Figure 3a′). The anlagen of the obliqui ventrales 1–3 (Figures 4a–4c) are distinct compact cell masses adjacent to the ventral ends of branchial arches 1–3 as inferred from histological sections.

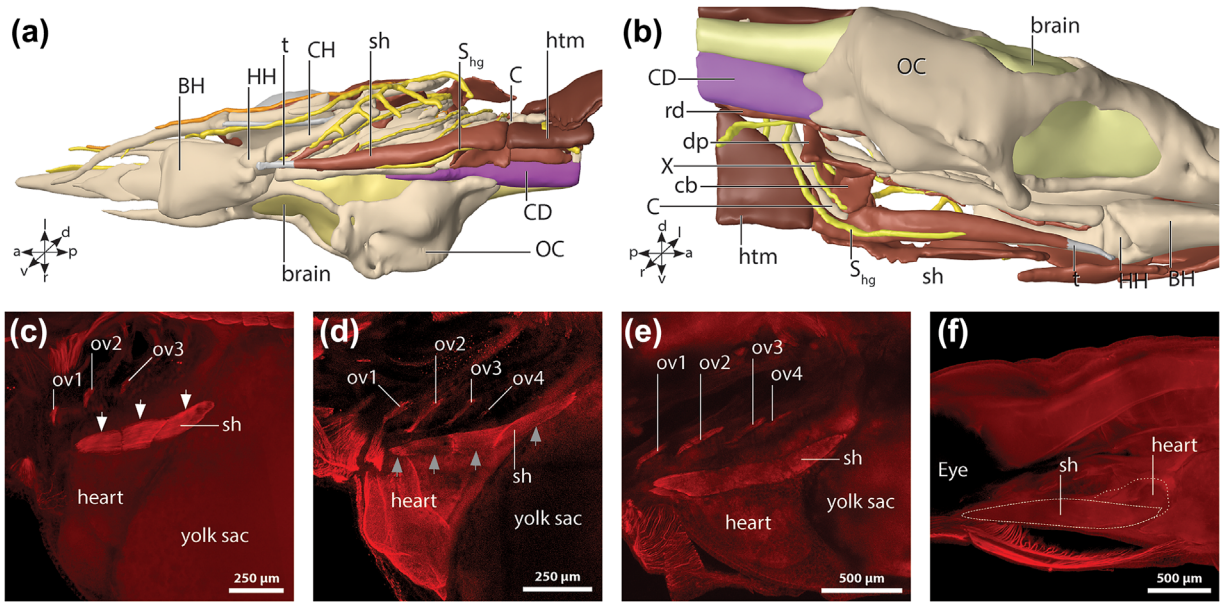

FIGURE 1 (a–b) 3D reconstruction of a µCT scan of a juvenile 22 mm *L. osseus* (VIMS 22687). (a) Ventral view. (b) Medial view. Muscles and nerves are reconstructed on the left side, while the skeletal elements are reconstructed in total. The different structures have been colored as follows: nerves, yellow to orange; brain, light yellow; muscles, dark flesh; skeletal elements, beige; chorda dorsalis, violet. (c–f) Maximum intensity projections of whole mount antibody stainings of *L. osseus* larvae. The ventral branchial region is shown from a lateral view. Muscles are colored in red. (c) Stage 30 (VIMS 22688). (d) Stage 31 (VIMS 22688). (e) Stage 32 (VIMS 22688). (f) Stage 33 (VIMS 22688). X, vagal nerve; a, anterior; BH, basihyal toothplate (Grande, 2010); C, cleithrum; cb, coracobranchialis; CD, chorda dorsalis; CH, ceratohyal; d, dorsal; dp, dilatator pharyngeus; HH, hypohyal; htm, hypaxonic trunk muscles; l, left; OC, otic capsule; ov1-ov4, obliquus ventralis 1-4; p, posterior; r, right; rd, retractor dorsalis; S_{hg}, spinal hypoglossal nerve; sh, sternohyoideus; t, tendon of the sternohyoideus; v, ventral

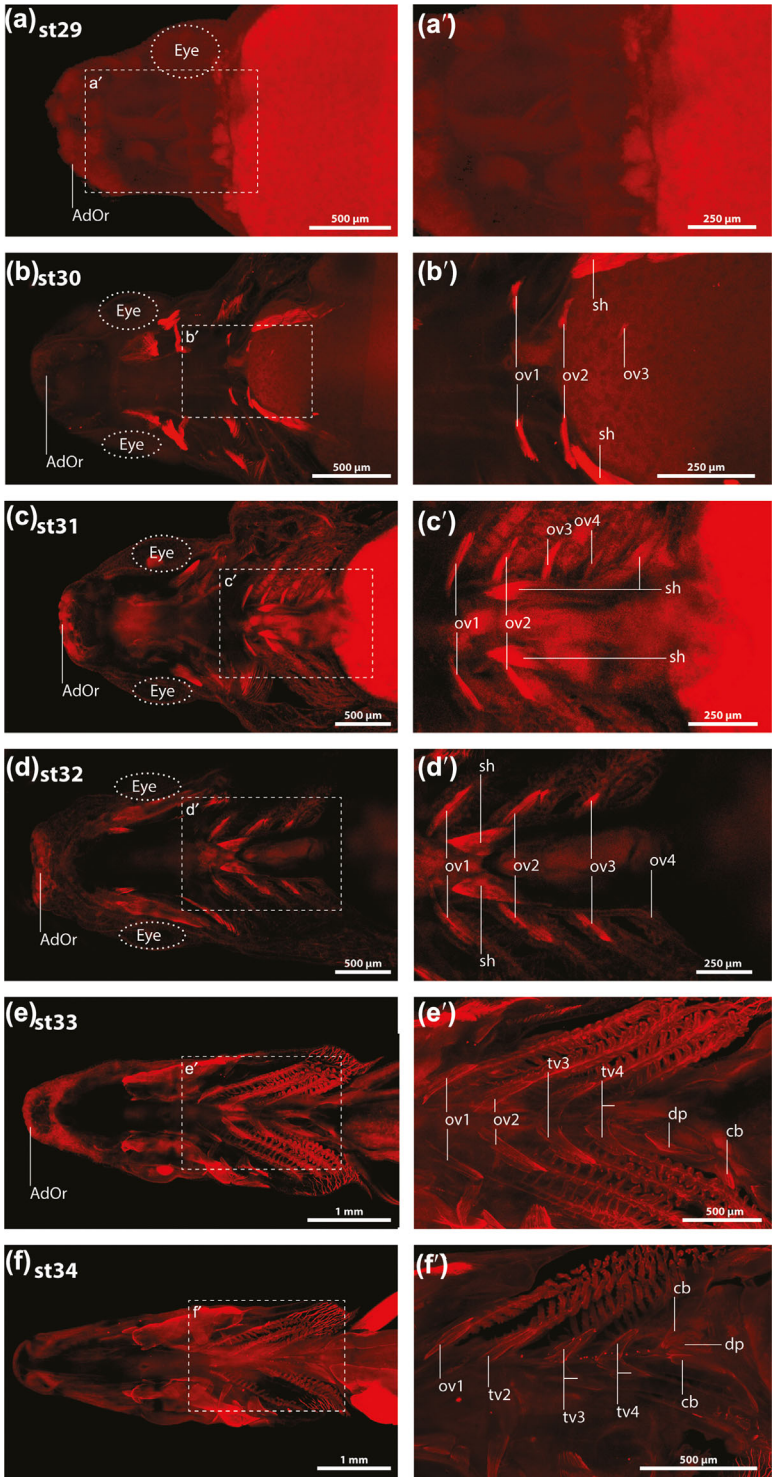

FIGURE 2 Maximum intensity projections of whole mount antibody staining of *L. osseus* larvae from a ventral view. Muscles are depicted in red. (a) Stage 29 (VIMS 22688). (a′) Close-up of the area marked by the dashed line in (a). (b) Stage 30 (VIMS 22688). (b′) Close-up of the area marked by the dashed line in (b). (c) Stage 31 (VIMS 22688). (c′) Close-up of the area marked by the dashed line in (c). (d) Stage 32 (VIMS 22688). (d′) Close-up of the area marked by the dashed line in (d). (e) Stage 33 (VIMS 22688). (e′) Close-up of the area marked by the dashed line in (e). (f) Stage 34 (VIMS 22688). (f′) Close-up of the area marked by the dashed line in (f). AdOr, adhesive organ; cb, coracobranchialis; dp, dilatator pharyngeus; ov 1–4, obliquus ventralis 1–4; sh, sternohyoideus; tv 2–4, transversus ventralis 2–4

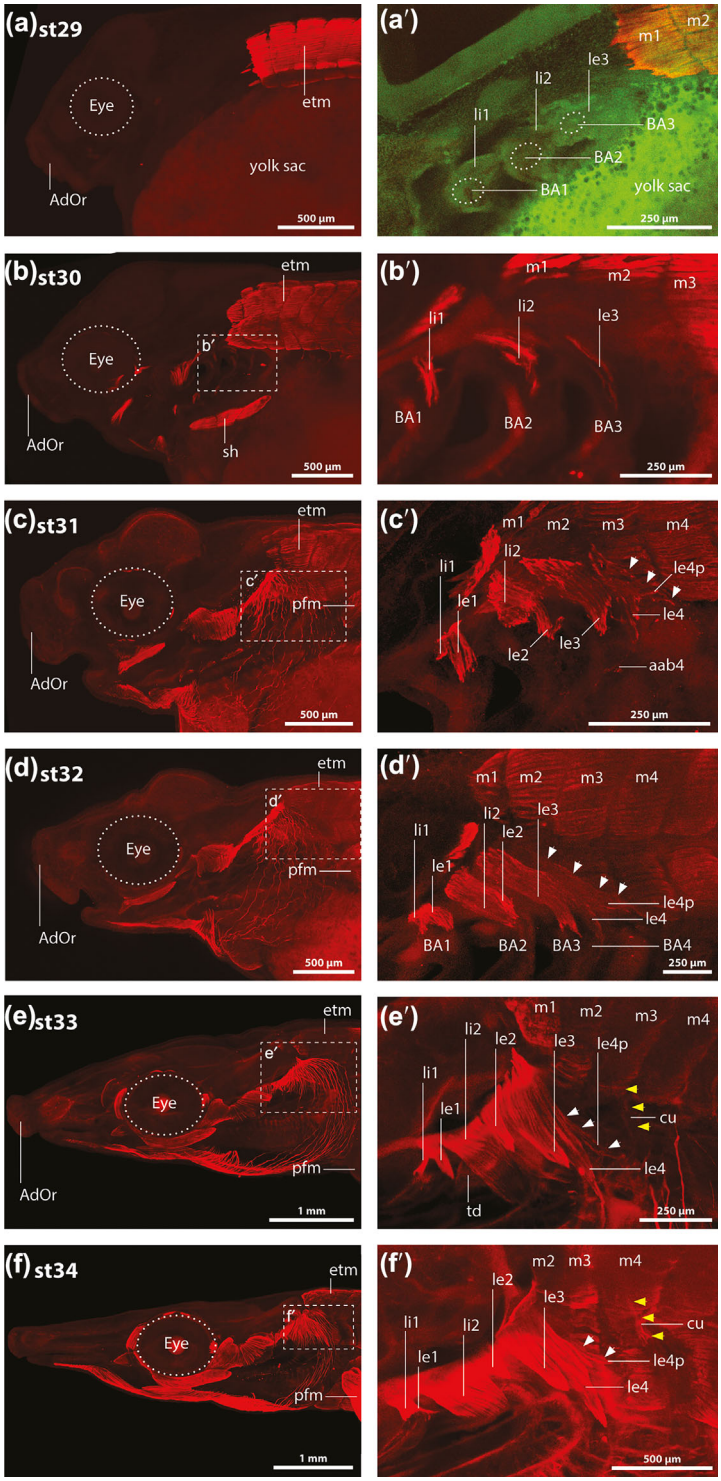

FIGURE 3 Maximum intensity projections of whole mount antibody stainings of the same *L. osseus* larvae as in Figure 2 from a lateral view. Muscles are depicted in red. (a) Stage 29 (VIMS 22688). (a′) Dorsolateral view of the brachial arches of the same specimen depicted in (a) Using autofluorescence of the tissue at 488 nm (green). (b) Stage 30 (VIMS 22688). (b′) Close-up of the area marked by the dashed line in (b). (c) Stage 31 (VIMS 22688). (c′) Close-up of the area marked by the dashed line in (c). (d) Stage 32 (VIMS 22688). (d′) Close-up of the area marked by the dashed line in (d). (e) Stage 33 (VIMS 22688). (e′) Close-up of the area marked by the dashed line in (e). (f) Stage 34 (VIMS 22688). (f′) Close-up of the area marked by the dashed line in (f). White arrows indicate the posterior portion of the levator externus 4. Yellow arrows indicate the cucullaris. AdOr, adhesive organ; BA 1–4, branchial arch 1–4; cu, cucullaris; etm, epaxonic trunk muscles; htm, hypaxonic trunk muscles; le 1–4, levator externus 1–4; le4p, posterior portion of the levator externus 4; li 1–2, levator of internus 1–2; m 1–4, myotome 1–4; pfm, pectoral fin muscles; td, transversus dorsalis

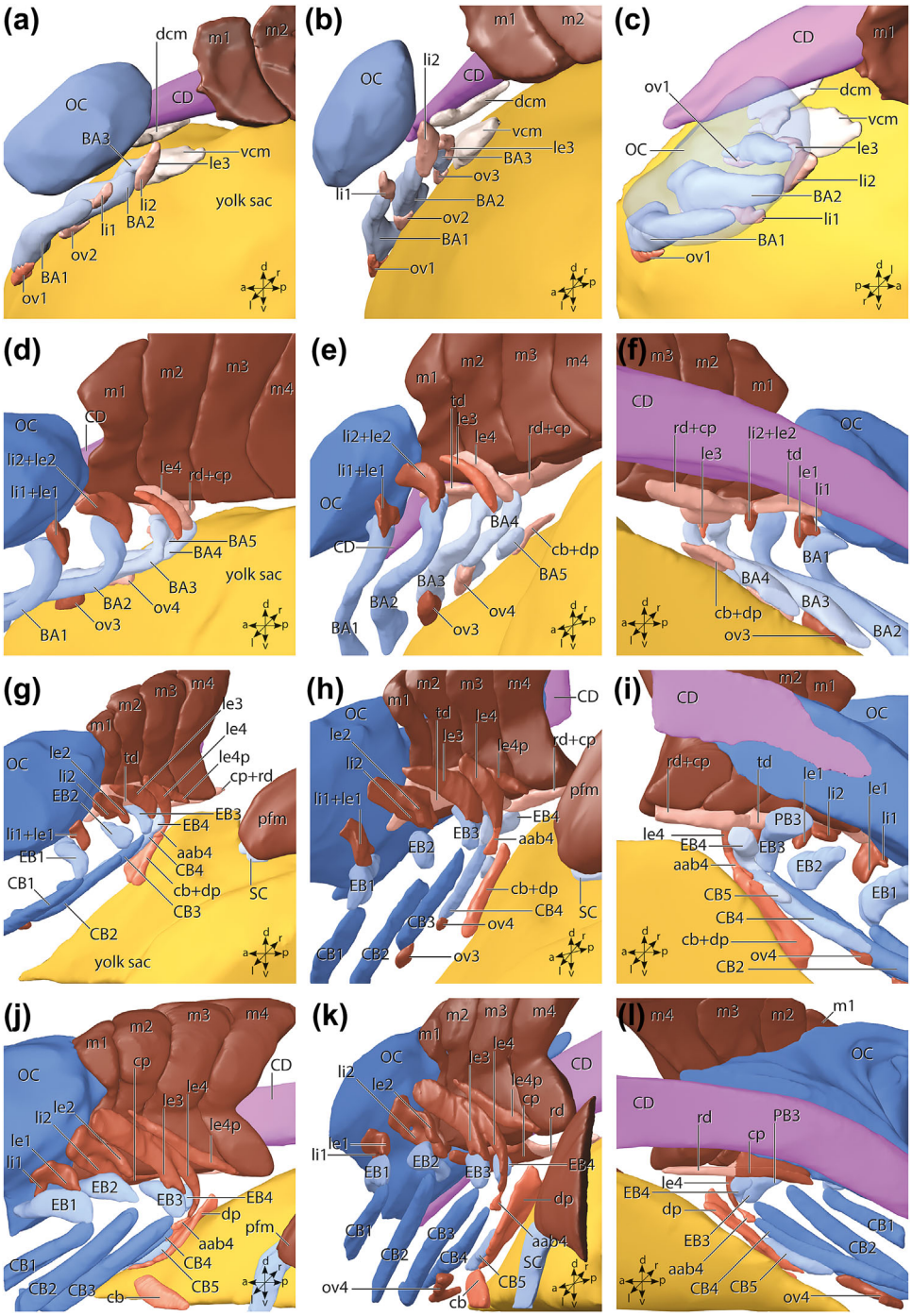

FIGURE 4 3D reconstructions based on fluorescent whole mount antibody stainings of *L. osseus* larvae. The different structures have been color as follows: Yolk, yellow; chorda dorsalis, violet; trunk muscles, brown; undifferentiated muscle anlagen, light flesh; differentiating muscles already showing some muscle fibers, flesh; differentiated muscles, dark flesh; cartilage anlagen, light blue; differentiating cartilage, blue; differentiated cartilage, dark blue; undifferentiated cell mass, light beige. (a–c) Stage 29 (VIMS 22688). (a) Lateral view. (b) Posterolateral view. (c) Dorsal view, the otic capsule has been made transparent. (d–f) Stage 30 (VIMS 22688). (d) Lateral view. (e) Posterolateral view. (f) Medial view. (g–i) Stage 31 (VIMS 22688). (g) Lateral view. (h) Posterolateral view. (i) Medial view. (j–l) Stage 32 (VIMS 22688). (j) Lateral view. (k) Posterolateral view. (l) Medial view. a, anterior; aab4, attractor arcus branchialium 4; BA1-BA5, branchial arch 1–5; cb, coracobranchialis; CB1-CB5, ceratobranchial 1–5; CD, chorda dorsalis; cp, constrictor pharyngeus; d, dorsal; dcm, dorsal cell mass; dp, dilatator pharyngeus; EB1-EB4, epibranchial 1–4; le1-le4, levator externus 1–4; le4p, posterior portion of the levator externus 4 (cucullaris *sensu* Edgeworth, 1911); l, left; li1-li2, levator internus 1–2; m1-m4, myotome 1–4; OC, otic capsule; ov1-ov4, obliquus ventralis 1–4; p, posterior; pfm, pectoral fin muscles; r, right; rd, retractor dorsalis; td, transverus dorsalis; v, ventral

At stage 30 (Figure 2b), the obliqui ventrales 1–3 are thin fiber bands attached to the ventral surface of the respective ceratobranchial anlagen (Figure 2b′). The anlage of the obliquus ventralis 4 (Figures 4d and 4e) is a small population of myoblasts located in the ventral area of the fourth branchial arch. A second distinct population of myoblasts is present at the ventral surface of the fifth branchial arch and adjacent to the myoblasts surrounding the pharynx (Figure 4f). We interpret this cell mass as the anlage of the coracobranchialis and dilatator pharyngeus muscles.

At stage 31 (Figure 2c), the obliquus ventralis 1 is elongated and reaches its insertion point at the anterior end of the basibranchial copula (Figure 2c′). The obliqui ventrales 2 and 3 are elongated too, but do not reach the basibranchial copula (Figure 2c′). The obliquus ventralis 4 has formed muscle fibers (Figure 2c′). The common anlage of the coracobranchialis and dilatator pharyngeus is elongated in anteroventral and posterodorsal direction (Figures 4g–4i) and the first muscle fiber formation is evident by a weak antibody signal. The anterior part of the anlage is slightly bent posteriorly. This part will form the coracobranchialis muscle.

At stage 32 (Figure 2d), all obliqui ventrales muscles are curved in a sharper angle to the basibranchial copula due to the elongation of the snout (Figure 2d′). The common anlage of the coracobranchialis and dilatator pharyngeus is divided into two distinct muscles (Figures 4j–4l). The anterior end of the coracobranchialis muscle points toward the developing ceratobranchial 5 and the posterior end toward the developing scapulocoracoid (Figure 4j).

At stage 33 (Figure 2e), the obliquus ventralis 2 has reached the medial side of the basibranchial. The obliqui ventrales 3 and 4 have met their antimeres and form per definition the transversi ventrales 3 and 4 now (Figure 2e′).

At stage 34 (Figure 2f) the obliquus ventralis 1 and the transversi ventrales 2–4 are in an increased pointed angle to the branchial midline correlated with the advanced elongation of the snout in juvenile *L. osseus* (Figures 2f′ and 2f″).

3.3 | Development of the dorsal branchial and pectoral muscles

At stage 29 (Figure 3a), dense cell areas are present, dorsal to the first three branchial arches. We interpret these cells as the anlagen of the levatores interni 1 and 2 and the levator externus 3 (Figure 3a′). The muscle anlagen adhere to the posterodorsal end of the corresponding branchial arch (Figures 4a–4c).

At stage 30 (Figure 3b) the anlagen of the levator muscles of the anterior three branchial arches, levator internus 1 and 2 and the levator externus 3, are distinct (Figure 3b′). Muscle fibers are already present in all three levator muscles. The levator externus 3 is less developed than the first two levatores and consists of only a few differentiated muscle fibers (Figure 3b′). All three muscles are attached to the posterodorsal surface of the corresponding branchial arch (Figures 4d and 4e). The levator externus 4 still consists of a small mass of myoblasts at the dorsal area of the fourth branchial arch and can be seen in histological sections as well as scans with a high laser intensity. The skeletal elements of the first and second branchial arches show first signs of chondrification. The third and fourth arches still appear as a dense mass with little extra-cellular matrix (Figures 4d–4f). A muscle anlage is present anteroventral to the first myomere, representing the anlage of the transversus dorsalis muscle (Figure 4f). Another muscle anlage is located ventrolateral to the chorda dorsalis. It starts at the level of myomere one and continues posteriorly until the level of myomere 3 (Figures 4e and 4f). Its anterior part consists of a population of myoblasts extending from the branchial arches in a medial direction and meets the anlage of its antimere in the midline ventral to the chorda dorsalis. Due to its position between branchial arches 2 and 3, we interpret the anterior part as the anlage of the transversus dorsalis and the posterior part as the anlage of the retractor dorsalis and constrictor pharyngeus muscle (Figures 4d–4f). The anlage appears continuous and no signs of segmentation are recognizable.

At stage 31 (Figure 3c), the levator internus 1 of the first branchial arch has reached its point of origin at the lateroventral surface of the otic capsule. The levator externus 1 has split from the levator internus 1 and inserts distally on epibranchial 1 (Figures 3c′, 4g, and 4h). The levator internus 2 approaches the otic capsule but does not insert on it yet. Its posterior end extends posteroventrally. It inserts on the epibranchial two forming the levator externus 2 (Figures 3c′, 4g, and 4h). It is a more massive muscle, compared to the previous stage (Figure 3c′). The levator externus 3 is broader compared to the previous stage (Figure 3c′). In close connection to the levator externus 3, the anlage of levator externus 4 has formed the first muscle fibers (Figure 3c′) and extends ventrally, reaching the area where the epibranchial 4 and ceratobranchial 4 will be in contact. This extension represents the anlage of the attractor arcus branchialium 4 (Figures 3c′ and 4h). Another muscle appears, originating from the levator externus 4 and running posteroventral into the direction of the developing shoulder girdle (Figure 3c′, white arrows). We call this muscle the posterior portion of the levator externus 4.

At stage 32 (Figure 3d) the levatores internus and externus two have reached their point of origin at the surface of the otic capsule, posterodorsal to the first levator muscle (Figures 3d′, 4j, and 4k). The posterior portion of the levator externus 4 has become broader and extends farther posteriorly (Figure 3d′). Its anterior end seems separate from the fourth branchial levator in the specimen used for the 3D reconstruction (Figure 4j) but appears connected in another specimen of almost the same size, and in larvae of later stages. The

posterior portion of the levator externus 4 is innervated by a ramus of the vagal nerve exiting the posterior vagal ganglion close to the vagal ramus of the fourth branchial arch (Figure 5). First muscle fibers are present in the anlage of the transversus dorsalis. The common anlage of the constrictor pharyngeus and retractor dorsalis muscles shows an anterior-to-posterior differentiation. Its anterior part shows first muscle fibers, while its posterior part still consists of myocytes (Figures 4k and 4l).

At stage 33 (Figure 3e), all the dorsal muscles of the branchial arches are present. The attractor arcus branchialium 4 has split from the ventral end of the fourth levator muscle, bridging the joint between epi- and ceratobranchial 4 (Figure 6a). The transversus dorsalis has formed more muscle fibers (Figure 3e′). The posterior portion of the levator externus 4 ends in the lateral skin (Figure 3e′). Posterodorsally, the anlage of the cucullaris appears close to the developing cleithrum and already shows muscle fiber formation (Figure 3e′, yellow arrows; Figure 6a).

At stage 34 (Figure 3f), the dorsal levator muscles as well as the attractor arcus branchialium 4 show no differences compared to older specimens (Figure 3f′). The posterior portion of the levator externus 4 is smaller compared to earlier stages but still inserts in the skin anterior to the pectoral girdle (Figure 3f′, white arrows; 6B, C, green arrows). The cucullaris has formed more muscle fibers (Figures 3f′, 6d, and 6f) and is attached to the occiput via a dorsal fascia in juveniles older than stage 34 (Figure 6f, also shown in Figure 7a). The ramus accessorius of the vagal nerve runs posterodorsally and innervates the cucullaris muscle (Figure 6g). A complete innervation scheme of all the branchial muscles, derived from whole mount antibody stainings as well as histological sections, is given in Figure 5.

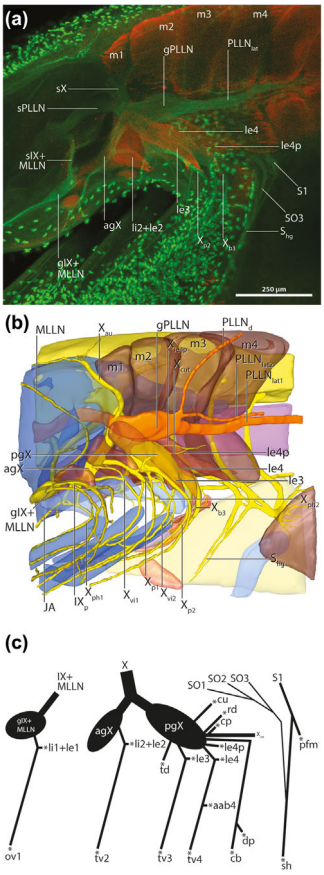

FIGURE 5 Maximum intensity projections of a whole mount antibody staining of a *L. osseus* larva at stage 32 (VIMS 22688). The posterior branchial region is shown from a lateral view. Muscles are depicted in red, nerves are depicted in green. (b) 3D reconstruction of the same data set as shown in (a). Coloring as described for Figure 4, nerves are depicted in yellow to orange. Muscles and skeletal elements have been made transparent to show the underlying nerves. (c) Innervation scheme of the branchial and anterior pectoral muscles deduced from Whole mount antibody stainings as well as histological sections. IX + MLLN, glossopharyngeal and middle lateral line nerve; IX_p, post-trematic ramus of IX; X, vagal nerve; X_{au}, ramus auricularis of X; X_{b3}, branchial ramus 3 of X; X_{cut}, cutaneous ramulus of X; X_{in}, ramus intestinalis of X; X_{le4p}, X motor ramus innervating the posterior portion of the levator externus 4; X_{p1}-X_{p2}, post-trematic ramus 1–2 of X; X_{ph1}-X_{ph2}, pharyngeal ramus 1–2 of X; X_{vi1}-X_{vi2}, visceral ramus 1–2 of X; aab4, attractor arcus branchialium 4; agX, anterior vagal ganglion; cb, coracobranchialis; cp, constrictor pharyngeus; cu, cucullaris; dp, dilatator pharyngeus; gIX + MLLN, ganglion of the glossopharyngeal and middle lateral line nerve; gPLLN, ganglion of the posterior lateral line nerve; le1-le4, levator externus 1–4; le4p, posterior portion of the levator posterior 4; li1-li2, levator internus 1–2; m1-m4, myotome 1–4; MLLN, middle lateral line nerve; ov1, obliquus ventralis 1; pfm, pectoral fin muscles; pgX, posterior ganglion of the vagal nerve; PLLN, posterior lateral line nerve; $PLLN_d$, darsal ramus of PLLN; $PLLN_{lat1}$-$PLLN_{lat2}$, lateral ramus 1–2 of PLLN; rd, retractor dorsalis; sIX + MLLN, stem of IX and MLLN; sX, stem of X; S1, spinal nerve 1; SC, scapulocoracoid; sh, sternohyoideus; SO1-SO3, spino-occipital nerve 1–3; sPLLN, stem of the PLLN; td, transversus dorsalis; tv2-tv4, transversalis ventralis 2–4

4 | DISCUSSION

4.1 | Development of the hypobranchial musculature

The sternohyoideus is the only hypobranchial muscle present in *L. osseus*. Edgeworth (1935) reported that the muscle has seven to nine "inscriptions," implying an origin from seven to nine anterior somites. In contrast to Edgeworth's finding, we found that the sternohyoideus muscle consists of three to four segments. An origin from the anterior-most three to four somites gains further support from our observation on the composition of the spinal hypoglossal nerve. Three spino-occipital nerves exit the occiput through distinct foramina and fuse to form a single nerve. In turn, this compound nerve becomes accompanied by fibers from the first spinal nerve (Figures 5b and 5c) which might increase the sensory component of the spinal hypoglossal nerve (Edgeworth, 1935). An innervation of the sternohyoideus, consisting of

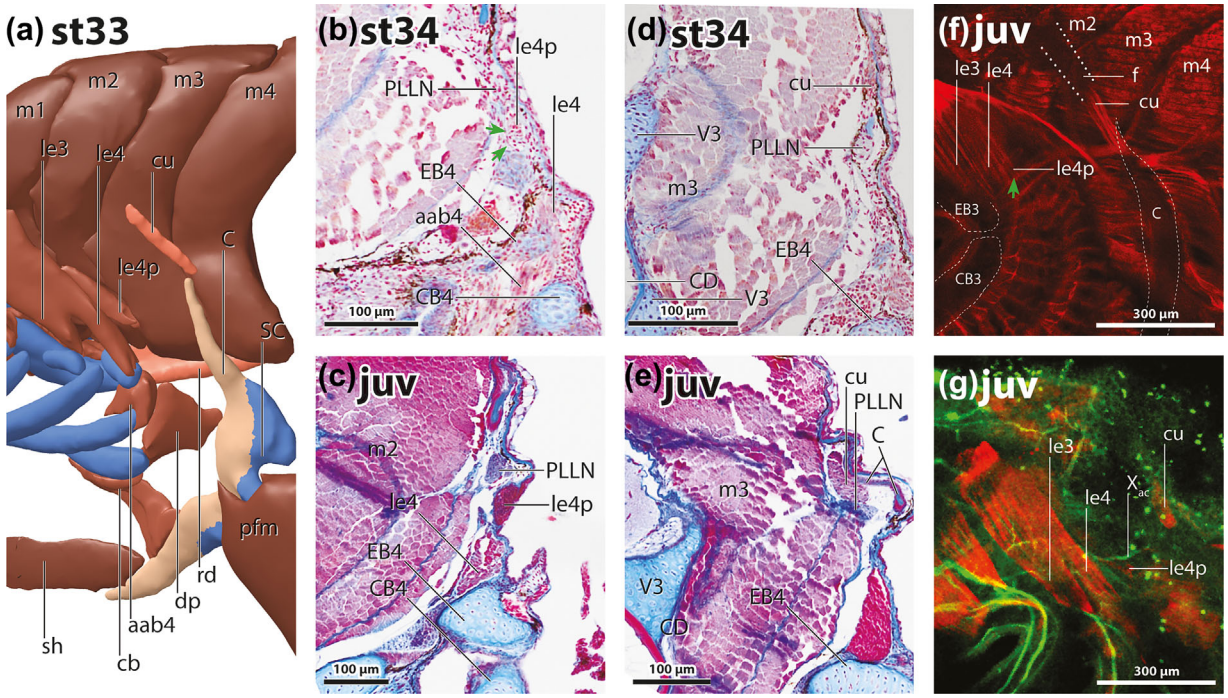

FIGURE 6 (a) 3D reconstruction based on fluorescent whole mount antibody staining of *L. osseus* larva at stage 33 (VIMS 22688). The posterior branchial region and the pectoral girdle are shown from a posterolateral view. Coloring as described for Figure 4, the ossified cleihtrum is colored in beige. (b–e) Histological section through the posterior branchial region of *L. osseus* larvae. (b and d) Stage 34 (LoSec003). (c and e) Juvenile (27 mm, LoSec005). (f) (20.0 mm, VIMS 22688) and (g) (22.0 mm, VIMS 22688), Maximum intensity projections of whole mount antibody stainings of a juvenile *L. osseus.* The position of skeletal elements and the fascia is indicated by dotted lines. Muscles are depicted in red, nerves are depicted in green. Green arrows indicate the posterior portion of the levator externus 4. X_{ac}, ramus accessories of the vagal nerve; aab4, attractor arcus branchialium 4; C, cleihtrum; cb, coracobranchialis; CB3-4, ceratobranchial 3-4; CD, chorda dorsalis; dp, dilatator pharyngeus; EB3-4, epibranchial 3- 4; f, fascia; le3-4, levator externus 3-4; le4p, posterior portion of the levator externus 4; m1-m4, myotome 1-4; pfm, pectoral fin muscles; PLLN, posterior lateral line nerve; rd, retractor dorsalis, V3, vertebra 3

three to four muscular segments, correlates with the observed composition of the spinal hypoglossal nerve by three spino-occipital and one spinal nerve. Fate mapping experiments in actinopterygians, similar to tetrapods (Piekarski & Olsson, 2007; Theis et al., 2010) are needed to draw the final conclusion of how many somites form the sternohyoideus in *L. osseus*.

4.2 | Development of the branchial muscles

As described by Edgeworth (1911, 1929, 1935), we also found a single dorsal and ventral muscle anlage (muscle plate in Edgeworth, 1935) for each branchial arch (Figures 4a–4c). These anlagen give rise to the levatores interni and externi dorsally and the obliqui ventrales ventrally (Edgeworth, 1911, 1935). Furthermore, we were able to describe developmental stages of *L. osseus* in which the attractor arcus branchialium 4 is still connected to the levator externus 4 (Figures 4g–4l), confirming the origin of the attractor from this branchial levator muscle (Edgeworth, 1929). We also confirm Edgeworth's description of the developmental pattern of the ventral branchial muscles. As stated by Edgeworth (1911, 1935) they begin to develop as obliqui ventrales. As development proceeds, the second to fourth obliqui ventrales alter their orientation, grow toward the branchial mid-line and fuse to their antimeres forming transversi ventrales (Figure 2).

4.3 | Development of the cucullaris muscle

Previous information on the cucullaris muscle in *Lepisosteus* is conflicting. Edgeworth (1935) reported a cucullaris originating from the levator externus 4 in *Lepisosteus* (probably also *L. osseus*). According to Edgeworth (1935), it forms directly posterior the levator externus 4, running posteriorly and ending in the skin without attaching to the pectoral girdle. Norris (1925) in contrast described a cucullaris in *L. osseus*, originating from the occipital fascia, running posteriorly and inserting on the cleithrum. Other authors (Greenwood & Lauder, 1981; Jessen, 1972) reported the absence of the cucullaris muscle in some *Lepisosteus* species including *L. osseus*. Our results show that the muscle interpreted as the cucullaris by Edgeworth (1911) in *Lepisosteus* is a posterior portion of the levator externus 4 (Figures 3c′, 4g, and 4h) and probably was misidentified because of (1) its origin (together

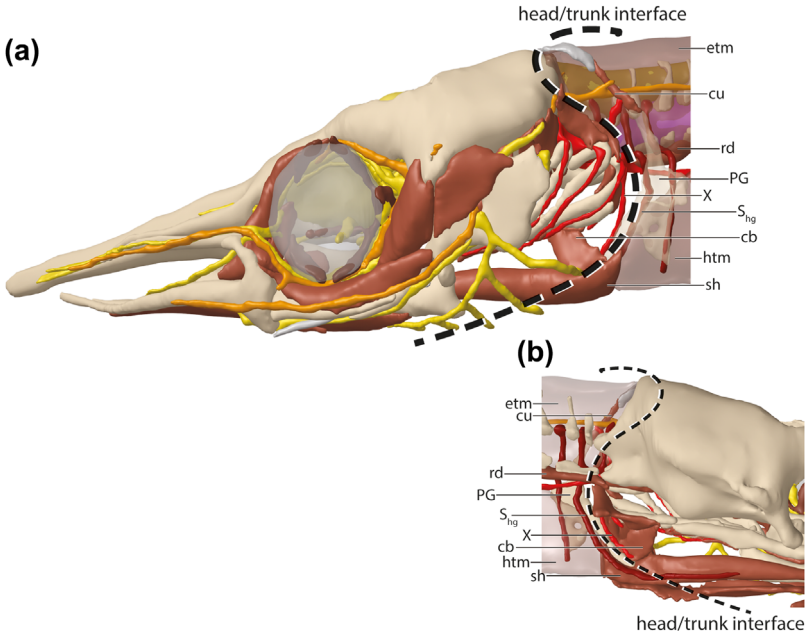

FIGURE 7 The same 3D reconstruction as shown in Figure 1 (VIMS 22687). Coloring as described for Figure 1. The dashed line indicates the head/trunk interface, outlined by the vagal (light red) and spinal hypoglossal (dark red) nerves. The head-derived cucullaris and retractor dorsalis muscles extend into the trunk, crossing the head/trunk interface, while the coracobranchialis muscle is situated anterior to that interface. (a) Lateral view. (b) Median view of the posterior branchial region. X, vagal nerve; cb, coracobranchialis; cu, cucullaris; PG, pectoral girdle; rd, retractor dorsalis; S_{hg}, spinal hypoglossal nerve; sh, sternohyoideus

with the levator externus 4) at the otic capsule and posteriorly directed course and (2) the absence of the "real" cucullaris muscle in the specimens studied by Edgeworth (1911) due to the delayed differentiation of the cucullaris compared to the other head muscles. The muscle we identified as the cucullaris muscle in *L. osseus* is congruent with the description of this muscle by Norris (1925). He determined the cucullaris based on its origin and insertion as well as the innervation by the vagal nerve. Because he did not observe the posterior portion of the levator externus 4 in his specimens, the conclusion that the cucullaris muscle develops from the levator externus 4 (Edgeworth, 1911) could not be refuted. The reported absence of the cucullaris in some specimens investigated by Jessen (1972) could be due to the inconspicuousness of this delicate muscle in or its reduction in larger animals. We show that the cucullaris and the posterior portion of the levator externus 4 as described by Edgeworth (1911) are present simultaneously but independent from each other (Figure 3e′, f′, and 6a) in *L. osseus* from stage 35 on to early juveniles. We never observed a connection between them in any of our specimens. Our investigation clarifies the identity of the cucullaris. and also disproves Edgeworths statement about the first appearance of the cucullaris muscle in synchrony with the levator externus 4 in *L. osseus*. However, important questions remain. (1) What is the function and evolutionary significance of the posterior portion of the levator externus 4? (2) What is the embryonic origin of the cucullaris and why does it form so late (see hypothesis below)?

4.4 | The retractor dorsalis muscle

According to Edgeworth (1929, 1935), in *Lepisosteus* the retractor dorsalis originates from the constrictor pharyngeus and is therefore of cranial origin, whereas other authors (Allis, 1897; Wiedersheim & Weismann, 1904) reported an origin from the trunk myotomes. Interestingly, all authors reported an innervation by the vagal nerve, while an origin from trunk myotomes (Wiedersheim & Weismann, 1904) would imply a spinal innervation. Our observation concurs with Edgeworth that the muscle is a derivative of the constrictor pharyngeus and therefore of cranial origin (Figure 4f).

Further, we observed a delay in muscle fiber formation within the retractor dorsalis portion compared to the constrictor pharyngeus portion (Figure 4l). This delayed timing of the muscle fiber development resembles the delayed fiber formation in the cucullaris. It is conspicuous, that the retractor dorsalis of *Lepisosteus* shows a developmental pattern very similar to that of the cucullaris muscle and therefore raises the same question: Why does it form so late?

4.5 | Developmental pattern of the muscles in the head/trunk interface

The trunk myogenic program is activated early in development (Theis et al., 2010). It promotes the differentiation of trunk-derived muscles (e.g., the hypobranchial musculature) via the expression of *Pax3* but inhibits differentiation of

head-derived muscles (Mootoosamy & Dietrich, 2002; Sambasivan, Kuratani, & Tajbakhsh, 2011; Tzahor et al., 2003). In the head, the migrating neural crest cells activate head muscle differentiation by inhibiting myogenic suppressors such as *Wnts* and *BMPs* (Theis et al., 2010; Tzahor et al., 2003). To reach its attachment site on the pectoral girdle, the anlage of the cucullaris muscle has to grow out from the head into the trunk, crossing the head/trunk interface. Thereby, the cucullaris/trapezius changes from the head myogenic environment into the trunk myogenic environment (Theis et al., 2010). The trunk myogenic program inhibits differentiation of the cucullaris muscle until it is downregulated or migrating cranial neural crest cells reach the cucullaris anlage, promoting an activating stimulus (Theis et al., 2010). At the time when the cucullaris starts to form muscle fibers, all other head and trunk muscles are already differentiated (Ericsson et al., 2013; Theis et al., 2010).

By investigating the timing of the muscles developing in the head/trunk interface of *Lepisosteus*, we can test this "tetrapod-based" hypothesis using our data gained from a basal actinopterygian species. In *L. osseus* a coracobranchialis and a retractor dorsalis muscle connect the head to the trunk in addition to the hypobranchial and cucullaris muscles. Despite its insertion on the pectoral girdle, the coracobranchialis muscle does not cross the head/trunk interface outlined by the vagal and spinal hypoglossal nerve (Figures 7a and 7b). In contrast, the retractor dorsalis and the cucullaris, both innervated by the vagal nerve, originate from the head, cross the head/trunk interface and insert on structures situated in the trunk, like the third and fourth vertebrae (retractor dorsalis) or the cleithrum (cucullaris) (Figures 7a and 7b). Based on what is known in tetrapods (Theis et al., 2010), we propose, that the anlagen of the cucullaris and retractor dorsalis muscles are under the inhibiting influence of the trunk myogenic program (Figure 8a, green gradient). In the head, migrating cranial neural crest cells (Figure 8b) inhibit the trunk myogenic program, promoting the differentiation of the head muscles (Figure 8c, blue gradient within the branchial arches). In the posterior head region the circumpharyngeal crest cells migrate around the posterior-most branchial arch along the head/trunk interface (Figure 8c). They reach the coracobranchialis muscle, promoting its differentiation, but not the more posterior anlagen of the cucullaris and retractor dorsalis (Figure 8d). The late differentiation of these two muscles can be explained in two different ways. First, only a small population of cranial neural crest cells reaches the anlagen,

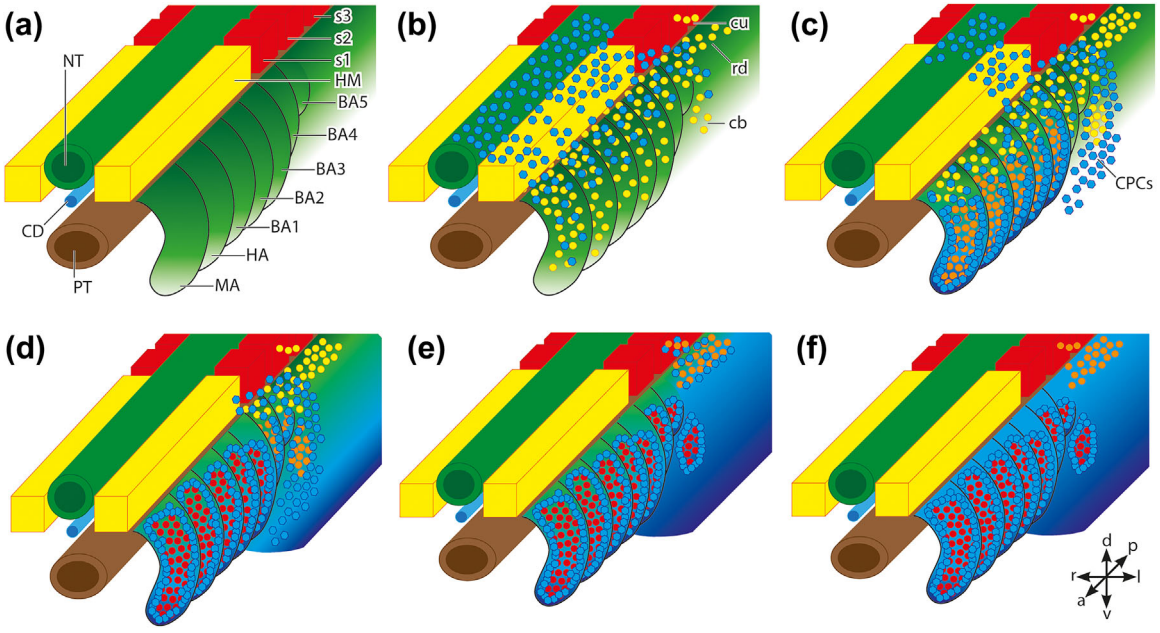

FIGURE 8 A possible explanatory scenario for the developmental pattern of the muscles of the head/trunk interface of *L. osseus*. (a–d) Show the successive progression from the early migration of the myogenic progenitor cells (myoblasts; yellow dots) and neural crest cells (blue hexagons) in the branchial arches. In the branchial arches, the myoblasts differentiate into myocytes (orange dots), which later form functioning muscle fibers (red dots). *Wnts* and *BMPs* genes (green gradient) are expressed from the neural tube and the overlaying ectoderm inhibiting head muscle formation. In the trunk the expression of *Pax3* initiates the trunk myogenic program unimpaired of *Wnts* and *BMPs*. In the branchial arches, *Wnt* and *BMP* inhibitors are expressed by neural crest cells (blue gradient), activating the head myogenic program. (e and f) Are two possible explanations, which could also act side-by-side, for the late differentiation of the cucullaris and retractor dorsalis muscle. The cross in the lower right corner shows the axis orientations (a, anterior; p, posterior; d, dorsal; v, ventral; l, left; r right). BA1 to 5, branchial arch 1–5; cb, coracobranchialis; CD, chorda dorsalis; CPCs, circumpharyngeal crest cells; cu, cucullaris; HA, hyoid arch; HM, head mesoderm; MA, mandibular arch; NT, neural tube; PT, pharyngeal tube; rd, retractor dorsalis

resulting in a slower inhibition of the trunk myogenic program (Figure 8e) or no neural crest cells reach the anlagen of the retractor dorsalis and cucullaris and muscle formation starts when the trunk myogenic program becomes down-regulated (Figure 8f). Fate mapping studies of the neural crest and anterior-most somites in basal actinopterygians as well as gene expression studies for *Pax3*, *Wnts*, and *BMPs* are needed to test this scenario.

Our results on the delayed differentiation of the cucullaris and retractor dorsalis muscles are similar to the pattern observed for the trapezius muscle in tetrapod taxa (e.g., Theis et al., 2010). We therefore speculate that the mechanisms underlying the developmental pattern of the muscles in the head/trunk interface might be conserved throughout, at least, the Osteichthyes.

ACKNOWLEDGMENTS

We would like to thank P. McGrath and E. Loose for their help in the field to collect and preserve larval and juvenile gars. We would like to thank Katja Felbel for help with histological sections. We are grateful to E. Hilton for supporting our research, offering his lab to us and for the countless discussions. We thank Sarah K. Huber for curatorial assistance. We also thank the two anonymous reviewers for valuable comments on the manuscript. The monoclonal antibodies obtained from the Developmental Studies Hybridoma Bank were developed under the auspices of the NICHD and maintained by The University of Iowa, Department of Biological Sciences, Iowa City, IA 52242, USA. This project was supported by the Volkswagen Foundation, Germany (project no. I84 / 825 to P Konstantinidis).

ORCID

Benjamin Naumann http://orcid.org/0000-0003-0970-2431

REFERENCES

Allis, E. P. (1897). The cranial muscles and first spinal nerves in *Amia calva*. *Journal of Morphology*, *12*, 487–772.

Böck, P. (1989). *Romeis mikroskopische technik*. München: Urban & Schwarzenberg.

Couly, G. F., Coltey, P. M., & Le Douarin, N. M. (1993). The triple origin of skull in higher vertebrates: A study in quail-chick chimeras. *Development*, *117*(2), 409–429.

Edgeworth, F. H. (1911). Memoirs: On the morphology of the cranial muscles in some vertebrates. *Journal of Cell Science*, *2*(222), 167–316.

Edgeworth, F. H. (1929). The development of some of the cranial muscles of ganoid fishes. *Philosophical Transactions of the Royal Society of London. Series B, Containing Papers of a Biological Character*, *217*, 39–89.

Edgeworth, F. H. (1935). *The cranial muscles of the vertebrates*. Cambridge: Cambridge University Press.

Epperlein, H. H., Khattak, S., Knapp, D., Tanaka, E. M., & Malashichev, Y. B. (2012). Neural crest does not contribute to the neck and shoulder in the axolotl (*Ambystoma mexicanum*). *PLoS ONE*, *7*(12), e52244. https://doi.org/10.1371/journal.pone.0052244

Ericsson, R., Cerny, R., Falck, P., & Olsson, L. (2004). Role of cranial neural crest cells in visceral arch muscle positioning and morphogenesis in the Mexican axolotl, *Ambystoma mexicanum*. *Developmental Dynamics*, *231*(2), 237–247. https://doi.org/10.1002/dvdy.20127

Ericsson, R., Knight, R., & Johanson, Z. (2013). Evolution and development of the vertebrate neck. *Journal of Anatomy*, *222*(1), 67–78. https://doi.org/10.1111/j.1469-7580.2012.01530.x

Fürbringer, M. (1874). Zur vergleichenden anatomie der schultermuskeln. II theil. *Jenaische Zeitschrift für Naturwissenschaften*, *8*, 175–280.

Gegenbaur, C. (1889). *Vergleichende Anatomie der Wirbelthiere: mit Berücksichtigung der Wirbellosen*. Leipzig: W. Engelmann.

Grande, L. (2010). An empirical synthetic pattern study of gars (Lepisosteiformes) and closely related species, based mostly on skeletal anatomy. The resurrection of Holostei. *Copeia*, *10*(2A), 1.

Greenwood, P. H., & Lauder, G. V. (1981). Protractor pectoralis muscle and the classification of teleost fishes. *Bulletin. Zoology series-British Museum (Natural History) Dept. of Zoology*.

Huang, R., Zhi, Q., Patel, K., Wilting, J., & Christ, B. (2000). Contribution of single somites to the skeleton and muscles of the occipital and cervical regions in avian embryos. *Anatomy and Embryology*, *202*(5), 375–383.

Jessen, H. L. (1972). Schultergürtel und Pectoralflosse bei Actinopterygiern [Shoulder girdle and pectoral fin in actinopterygians]. *Fossils and Strata*, *1*, 1–101.

Klymkowsky, M. W., & Hanken, J. (1991). Whole-mount staining of *Xenopus* and other vertebrates. *Methods in Cell Biology*, *36*, 419–441.

Kuratani, S. (1997). Spatial distribution of postotic crest cells defines the head/trunk interface of the vertebrate body: Embryological interpretation of peripheral nerve morphology and evolution of the vertebrate head. *Anatomy and Embryology*, *195*(1), 1–13.

Kuratani, S. (2008). Evolutionary developmental studies of cyclostomes and the origin of the vertebrate neck. *Development, Growth and Differentiation*, *50*(Suppl 1), S189–S194. https://doi.org/10.1111/j.1440-169X2008.00985.x

Long, W. L., & Ballard, W. W. (2001). Normal embryonic stages of the longnose gar, *Lepisosteus osseus*. *BMC Developmental Biology*, *1*, 6.

Matsuoka, T., Ahlberg, P. E., Kessaris, N., Iannarelli, P., Dennehy, U., Richardson, W. D., . . . Koentges, G. (2005). Neural crest origins of the neck and shoulder. *Nature*, *436*(7049), 347–355. https://doi.org/10.1038/nature03837

Metscher, B. D. (2009). MicroCT for comparative morphology: Simple staining methods allow high-contrast 3D imaging of diverse non-mineralized animal tissues. *BMC Physiology*, *9*, 11. https://doi.org/10.1186/1472-6793-9-11

Mootoosamy, R. C., & Dietrich, S. (2002). Distinct regulatory cascades for head and trunk myogenesis. *Development*, *129*(3), 573–583.

Noden, D. M. (1983). The embryonic origins of avian cephalic and cervical muscles and associated connective tissues. *American Journal of Anatomy*, *168*(3), 257–276. https://doi.org/10.1002/aja.1001680302

Oisi, Y., Fujimoto, S., Ota, K. G., & Kuratani, S. (2015). On the peculiar morphology and development of the hypoglossal, glossopharyngeal and vagus nerves and hypobranchial muscles in the hagfish. *Zoological Letters*, *1*, 6. https://doi.org/10.1186/s40851-014-0005-9

Piekarski, N., & Olsson, L. (2007). Muscular derivatives of the cranialmost somites revealed by long-term fate mapping in the Mexican axolotl (*Ambystoma mexicanum*). *Evolution and Development*, *9*(6), 566–578. https://doi.org/10.1111/j.1525-142X2007.00197.x

Sambasivan, R., Kuratani, S., & Tajbakhsh, S. (2011). An eye on the head: The development and evolution of craniofacial muscles. *Development*, *138*(12), 2401–2415. https://doi.org/10.1242/dev.040972

Sefton, E. M., Bhullar, B. A., Mohaddes, Z., & Hanken, J. (2016). Evolution of the head-trunk interface in tetrapod vertebrates. *Elife*, *5*, e09972. https://doi.org/10.7554/eLife.09972

Tada, M. N., & Kuratani, S. (2015). Evolutionary and developmental understanding of the spinal accessory nerve. *Zoological Letters*, *1*, 4. https://doi.org/10.1186/s40851-014-0006-8

Theis, S., Patel, K., Valasek, P., Otto, A., Pu, Q., Harel, I., . . . Huang, R. (2010). The occipital lateral plate mesoderm is a novel source for vertebrate neck musculature. *Development*, *137*(17), 2961–2971. https://doi.org/10.1242/dev.049726

Trinajstic, K., Sanchez, S., Dupret, V., Tafforeau, P., Long, J., Young, G., . . . Ahlberg, P. E. (2013). Fossil musculature of the most primitive jawed vertebrates. *Science*, *341*(6142), 160–164. https://doi.org/10.1126/science.1237275

Tzahor, E., Kempf, H., Mootoosamy, R. C., Poon, A. C., Abzhanov, A., Tabin, C. J., . . . Lassar, A. B. (2003). Antagonists of Wnt and BMP signaling promote the formation of vertebrate head muscle. *Genes & Development*, *17*(24), 3087–3099. https://doi.org/10.1101/gad.1154103

Wiedersheim, R., & Weismann, A. (1904). *Ueber das Vorkommen eines Kehlkopfes bei Ganoiden und Dipnoern: sowie über die Phylogenie der Lunge*. Verlag von Gustav Fischer.

Winterbottom, R. (1974). Descriptive synonymy of striated muscles of teleostei. *Proceedings of the Academy of Natural Sciences of Philadelphia*, *125*(12), 225–317.

Zhu, M., Ahlberg, P. E., Pan, Z., Zhu, Y., Qiao, T., Zhao, W., . . . Lu, J. (2016). A Silurian maxillate placoderm illuminates jaw evolution. *Science*, *354*(6310), 334–336. https://doi.org/10.1126/science.aah3764

Ziermann, J. M., & Diogo, R. (2013). Cranial muscle development in the model organism ambystoma mexicanum: Implications for tetrapod and vertebrate comparative and evolutionary morphology and notes on ontogeny and phylogeny. *Anatomical Record-Advances in Integrative Anatomy and Evolutionary Biology*, *296*(7), 1031–1048. https://doi.org/10.1002/ar.22713

How to cite this article: Naumann B, Warth P, Olsson L, Konstantinidis P. The development of the cucullaris muscle and the branchial musculature in the Longnose Gar, (*Lepisosteus osseus*, Lepisosteiformes, Actinopterygii) and its implications for the evolution and development of the head/trunk interface in vertebrates. *Evolution & Development*. 2017;1–14. https://doi.org/10.1111/ede.12239